THE UNIVERSITY OF MICHIGAN

College of Engineering

Department of Mechanical Engineering

Cavitation and Multiphase Flow Laboratory

Report No. UMICH-03371-6-T

ASYMMETRIC CAVITATION BUBBLE COLLAPSE

(Submitted for Publication to ASME)

by

T. M. Mitchell*
F. G. Hammitt**

Financial Support Provided by:

National Science Foundation
Grant No. GK-13081

March 1971

*Formerly Doctoral Candidate, Nuclear Engineering Dept. and Research Assistant, Cavitation and Multiphase Flow Laboratory, Mechanical Engineering Department, University of Michigan.

**Professor-in-Charge, Cavitation and Multiphase Flow Laboratory, Mechanical Engineering Department, University of Michigan.

ABSTRACT

Numerical results describing the asymmetric collapse of vapor bubbles in a viscous incompressible liquid for various cases of axial symmetry involving boundary conditions which prevent the maintenance of spherical symmetry are presented using a modified Marker-and-Cell (MAC) technique.

The cases studied include an originally slightly non-spherical bubble in an infinite static liquid at uniform pressure; originally stationary spherical bubbles in a pressure gradient, and in a liquid at uniform pressure close to a rigid wall; and finally an originally spherical bubble moving through an otherwise stationary liquid at uniform pressure.

In all those cases which involve originally spherical bubbles, the bubble collapses in such a way as to form a jet.

TABLE OF CONTENTS

LIST OF FIGURES

NOMENCLATURE

b_o	Initial Distance of Bubble Center from Wall
c	Sonic Velocity in Liquid
D	$\vec{\nabla} \cdot \vec{u}$
f	Centroid Migration
P	"Head" = Pressure/Density
p_c	Constant Internal Pressure
p_∞	Liquid Pressure Far From Bubble
$\bar{R}$	Average Bubble Radius
R_o	Initial Bubble Radius
r	Radial Coordinate
t	Time
U	Impact Velocity of Liquid Jet
$\vec{u}$	Velocity Vector
V_∞	Liquid Velocity Far from Bubble
z	Measure of Bubble Deformation
ρ_L	Liquid Density
ν	Kinematic Viscosity
σ	Dimensionless Pressure Gradient

SUPERSCRIPTS

$\dot{}$	Time Derivative
$'$	Dimensionless

I. INTRODUCTION

A detailed understanding of the collapse of cavitation bubbles under various asymmetric initial and boundary conditions is of fundamental importance in developing an understanding of the cavitation damage mechanism. Various earlier numerical studies in this area (1-4, e.g.) have assumed the damage accompanying cavitation is due to the "shock" wave produced in the liquid during the rebound of bubbles which have previously collapsed to a very small size with a high pressure within. More recently a growing body (5-7, e.g.) of both theoretical and experimental evidence points to asymmetric collapse, in which the liquid on one segment of the surface moves inward at a much higher velocity than the rest of the bubble wall, thus forming a narrow high velocity liquid jet, as the culprit. (The theories are not mutually exclusive.)

The aim of the present study was to use currently available numerical techniques with the large computers now available to trace models of individual cavitation bubbles as far into their collapse as possible under a number of asymmetric initial and boundary conditions which are similar to those found in various real flow situations. The particular problems investigated include: 1) an initially slightly non-spherical stationary bubble; 2) initially spherical, stationary bubbles in two different linear pressure gradients; 3) an initially spherical bubble moving relative to the surrounding liquid; and 4) an initially spherical stationary bubble near a solid wall.

II. ANALYSIS

The general problem is defined as follows: A mass of homogeneous, viscous* incompressible liquid surrounds a "bubble" which is

---

*A viscosity of 100x 60^{o}F water was used. A large value was selected to aid in stabilizing the calculation and because earlier calculations (3) have shown that viscosity does not importantly affect bubble collapse over radius ratios as used here.

assumed initially to have a hypothetical rigid wall (as a "ping-pong ball"). The bubble may be assumed to contain gas and/or vapor whose pressure follows an appropriate equation of state, but in the present cases the internal pressure is assumed to be zero or constant with time, (assumptions which are equivalent). Surface tension effects are neglected, although they may be added to the analysis with only a slight increase in complexity. Thermodynamic effects are also assumed negligible. Arbitrary initial and boundary conditions including initial bubble shape, pressure and velocity distributions in the liquid, and a free-slip or non-slip adjacent solid wall may be imposed; however, all such conditions must be axially symmetric. The hypothetical bubble wall is assumed annihilated instantaneously at time zero, collapse ensuing from that point. The goal is to determine the subsequent shape of the bubble, local bubble wall velocities, and the instantaneous pressure at various points in the liquid.

The method here used for solving the problem is a modification of the Marker-and-Cell (MAC) method developed at Los Alamos.[8, 9] The details of the technique are described fully in the Ph. D. dissertation of the first author;[10] a brief description follows.

The starting point is the general vector form of the incompressible hydrodynamic equations for continuity and conservation of momentum:

$$D \equiv \vec{\nabla} \cdot \vec{u} = 0 \tag{1}$$

$$\frac{\partial \vec{u}}{\partial t} = -(\vec{u} \cdot \vec{\nabla})\vec{u} - \vec{\nabla} P + \nu \nabla^2 \vec{u} \tag{2}$$

where $\vec{u}$ is the velocity vector, P = pressure/density = "Head" and ν is the kinematic viscosity. If the divergence of Eq. (2) is taken and the appropriate vector identities are applied, the result is

$$\frac{\partial}{\partial t}(\vec{\nabla} \cdot \vec{u}) = -\vec{\nabla} \cdot (\vec{\nabla} \cdot \vec{u}\vec{u}) - \nabla^2 P \tag{3}$$

Equations (2) and (3) along with the appropriate initial and boundary conditions form the hydrodynamic basis for the MAC solution.

Axial symmetry is assumed and Eqs. (2) and (3) are then written for a system of spherical coordinates, first in component differential equation form, then in finite difference form. Appropriate formulations are established for boundary conditions including the axis of symmetry, free surfaces, free-slip and no-slip walls, and the "infinite" liquid. The region of interest is discretized, as shown in Fig. 1, with the boundary cells also indicated. In addition to the Eulerian (fixed) grid, a series of massless marker particles are assigned to locations on the liquid-void interface. The purpose of the particles is to show which cells are on the liquid surface and to serve as an outline tracing the bubble surface motion over the history of the collapse.

The sequence of calculations has been described previously.[10,11] In brief, if the pressure and velocity distribution are known throughout the liquid at some time t, then the finite difference form of Eq. (2) is used to find the new values for the radial and tangential velocity components. Eq. (3) is then solved iteratively to determine the new pressure distribution. The velocity components of the marker particles are then calculated by position-interpolation from the nearest Eulerian grid components, and the new marker particle positions are determined after movement by increments equal to the product of the particle velocity and the time increment δt. The grid is then scanned to see whether the marker particle motion has filled (or emptied) any of the previously empty (or full) Eulerian cells; if so, those cells are incorporated (or excluded) in the succeeding Eulerian calculations. The cycle is then repeated.

The present technique differs considerably from a technique reported recently by Plesset and Chapman[7] for solving similar problems. The primary differences are: 1) the present technique includes the primary velocity components while Plesset-Chapman uses the velocity potential; 2) the present technique includes viscosity while the latter (Plesset-Chapman) is for inviscid flow; and 3) the present

analysis is written in spherical coordinates, the latter in cylindrical. With regard to (3), there are distinct advantages on either side. A spherical grid offers good resolution in the region of interest during the early stages of the collapse, i.e., in the vicinity of the bubble wall, and may tend to reduce machine instabilities associated with conditions at infinity. On the other hand, cylindrical coordinates allow a straightforward and simple description of flat rigid surface boundaries. Spherical coordinates also are less satisfactory for large bubble deformations, when a jet of liquid may approach the origin of coordinates, which is essentially a singularity.

Some direct comparisons will be made between our results and those of Plesset and Chapman in the next section. Both techniques have been employed to treat one common problem, the collapse of an initially spherical bubble whose center is (3/2) R_o (R_o is the initial radius) from a flat rigid wall.

III. RESULTS

A. Initially Non-Spherical Bubble

The first of the four specific problems examined here is the determination of the effect of small initial perturbations of the surface of an otherwise spherical bubble collapsing in an infinite static liquid at originally uniform pressure. Plesset and Mitchell showed previously [12] that such perturbations should grow as the collapse ensues, i.e., the spherical collapse is unstable. The present solution then was intended only to examine the effect of viscosity on such a collapse and to allow some confirmation of the validity of the present technique.

The initial wall profile is given by

$$R_o(\theta) = R_o + a_3 P_3(\cos\theta) + a_6 P_6(\cos\theta)$$

where R_o is the initial "mean" radius,

a_3 and a_6 both are initially set equal to $0.01\, R_o$,

and P_3 and P_6 are, respectively, the third and sixth Legendre polynomials.

Fig. 2 shows a plot of the initial deviation from spherical symmetry (actual deviations magnified ten times). The outermost profile in Fig. 3 shows the same profile without such magnification, appearing to be virtually spherical to the naked eye.

Fig. 3 also shows the bubble shape profile at subsequent times. A comparison of the history of the Legendre polynomial coefficients calculated from the profiles of Fig. 3 with the Plesset-Mitchell results[12] indicates the same pattern (oscillation in sign with both increasing frequency and increasing magnitude as $R/R_o \rightarrow 0$) but both frequency and magnitude appear to have been reduced, presumably by the viscous effects. The instability of the spherical surface is also confirmed in the later time profiles in Fig. 3.

One significant observation which can be made from comparison of Fig. 2 and profile f of Fig. 3 is as follows. There are outward protuberances in Fig. 2 at about 0, 120, and 180° from the upper vertical axis, while in Fig. 3 there are inward deviations from the spherical shape at the same angles, with the maximum deformation in both figures on the 0° axis. This behavior suggests the Monroe jet or shaped charge effect, well known from World War II explosives design.

B. Effects of Pressure Gradient on Initially Spherical Bubble

The second of the asymmetric problems is the effect of pressure gradients on the collapse of initially stationary, spherical bubbles. These results have been reported in brief previously by the present authors.[11] Gibson, in his recent Ph. D. thesis[13], established the importance of the dimensionless pressure gradient

$$\sigma = R_o \, dp/dz \quad / \quad (p_\infty - p_c)$$

where dp/dz = pressure gradient

p_∞ = pressure in liquid far from bubble

and p_c = initial bubble internal pressure = constant.

He found, theoretically (using a small perturbation technique) as well as experimentally, that substantial deformation of the spherical shape would occur during collapse only for $|\sigma| \gtrsim 10^{-2}$.

Two cases were calculated in the present analysis, $\sigma = 0.19$ and $\sigma = 0.57$. The former case coincides with both experimental and theoretical cases reported by Gibson, while both values are typical for bubbles collapsing in the cavitating venturi used in this laboratory. High speed motion pictures of such bubbles collapsing in the venturi pressure gradient were previously reported by Ivany, Hammitt and Mitchell.[4]

The bubble wall profile histories for the two cases are shown in Figs. 4 and 5. In both cases the early stages of the collapse are markedly spherical, although there is considerable migration of the centroid in the direction of the low pressure side and hence creation of a sizable Kelvin impulse (The Kelvin impulse $I = M\dot{x}_o + J$, where $M = 2/3\ \rho_L \pi R^3$ = "induced mass", $\dot{x}_o$ the bubble translational velocity, and J is a function of the deformation rate of the bubble). Also in both cases the bubble wall in the vicinity of the lower vertical axis, i.e., on the high pressure side, accelerates inward faster than the rest of the surface until an inward protuberance develops, marking the beginning of the high speed jet. As one would expect, the steeper pressure gradient, $\sigma = 0.57$, results in greater migration of the centroid and earlier formation of the jet.

Figs. 6 and 7 allow some numerical evaluation of Gibson's and the present authors' theoretical models in comparison with the former's experimental data for the $\sigma = 0.19$ case. The two quantities used for comparison (from Gibson's thesis[13]) are a measure of the eccentricity $z = (d_1 - d_2)/(d_1 + d_2)$, where d_1 and d_2 are the respective horizontal and vertical diameters, and a measure of the vertical centroid motion f, which is defined with the aid of the schematic in the upper left corner of Fig. 7 as $f = ((d_3 - R_o) - d_2/2) / R_o$, where $(d_3 - R_o)$ measures the distance from the top of the bubble to the original centerline and $d_2 / 2$ is

the present "mean" radius. There is good agreement between the present author's calculations and Gibson's calculations for a bubble which collapses from "rest" until the late stages of collapse (The latter's model is based on the assumption of only small perturbations from spherical and hence obviously becomes invalid at some point in those late stages.) The discrepancy between the present results and Gibson's experimental data is explained with the aid of the third theoretical curve in Figs. 6 and 7; i.e., the experimental bubbles were grown in the same pressure gradient in which they subsequently collapse. Gibson's second theoretical analysis included the expansion effects, whereas the present model does not.

In summary, Figs. 6 and 7 show what the profile histories had already indicated, a continuing increase in the bubble deformation with time, as well as continuous movement of the centroid from its original position in the direction of the low pressure side.

Another point which can be made from these calculations is illustrated by Fig. 8. Here the wall velocity for $\theta = 180^{o}$, i.e., the "jet" is plotted as a function of its radial position. The jet velocities in the two cases (σ = 0.19 and 0.57) do not differ very greatly from the Rayleigh spherically symmetric wall velocity for a corresponding radial shrinkage until $R/R_o < 0.3$, when they begin to lag substantially.

At the end of the calculation, for a collapsing pressure ($p_\infty - p_c$) of one atmosphere the jet has attained a velocity of 220 ft/sec for a contraction to $R/R_o = 0.2$, in cold water, and is still accelerating. One does not expect that the velocity will continue to increase strongly as the jet traverses the bubble interior since the pressure gradient inside the jet will tend rather to spread the jet than to continue to accelerate it. The recent calculations of Plesset and Chapman[7] have confirmed this last hypothesis.

Although jet velocities of the order of 200 to 300 ft/sec may seem low to cause cavitation damage, the corresponding water hammer

pressure for a rigid material and cold water p_{WH} (= $\rho_L cU$) in the latter case is approximately 20,000 psi. Furthermore, liquid impingement velocities of precisely that value, 300 ft/sec, have been observed to damage materials as hard as stellite in repeated impacts (Ref., e.g., Hancox and Brunton[14].)

C. Effects of Translatory Velocity on Initially Spherical Bubble

The third asymmetric problem arises from a common experimental observation, the presence of a relative ("slip") velocity between the liquid and the bubble. For example, this phenomenon has been observed in a cavitating venturi experiment reported by Ivany, Hammitt, and Mitchell[4] in which they found bubbles moving some 5 ft/sec faster through the venturi throat than the calculated liquid velocity of 75 ft/sec. Slip is also a common observation in boiling experiments. The calculation performed here is for an initially stationary and spherical bubble of 1 mm radius with a liquid velocity far from the bubble (i.e., "slip") of 5 ft/sec, and $(p_\infty - p_c)$ equal to one atmosphere. The initial pressure and velocity distributions are determined from the velocity potential for a liquid moving past a sphere

$$\phi = V_\infty (r \cos\theta + R_o^3 \cos\theta / 2r^2)$$

The bubble wall profile history is shown in Fig. 9. There is increasing slip in the given direction as collapse proceeds. Migration of the cavity occurs in the direction of the slip and there is flattening on the downstream (180^o) side with the beginnings of jet formation in the direction of slip. Both observations are exactly as expected from the Kelvin impulse discussion earlier, i.e., the initial bubble translatory momentum must be conserved through a combination of acceleration of the bubble centroid and the formation of a vortex system. Similare results were also obtained in a study of the same venturi flow by Yeh and Yang[15] using a small perturbation technique.

The present calculations of the bubble centroid velocity can be compared with the analogous data for the limiting case of a collapse retaining spherical symmetry. As previously discussed and evaluated in various cases by Chincholle[16] one would expect in the latter case that the translational velocity of the bubble centroid varies as the volume ratio $(R/R_o)^3$. The present results near the end of the calculation indicate a centroid velocity about half of the predicted value for a bubble collapsing spherically throughout, for a corresponding volume shrinkage. The remaining half of the initial Kelvin impulse is presumed to have been absorbed in the effects associated with the deformation of the bubble and into viscous dissipation.

Fig. 10 shows the radial component of the liquid velocity at the wall at 0, 90 and 180° as a function of time. For a bubble (of any initial size) collapsing in water with $(p_\infty - p_c)$ equal to one atmosphere, the jet velocity ($\theta = 180^\circ$) at the end of the present calculation is 227 ft/sec and is still increasing when the calculation is terminated due to difficulties as the liquid approaches the origin of coordinates.

There do not appear to be any experimental confirmations of this jet velocity evaluation because of the difficulty of isolating the slip velocity phenomenon from such other sources of asymmetries as pressure gradients and nearby rigid walls. Based on the present results, however, one can conclude that only a slight slip velocity between liquid and bubble produces a sufficient Kelvin impulse to add considerably to the deformation a bubble will undergo during collapse.

D. Effects of Adjacent Rigid Wall on Initially Spherical Bubble

The last of the four asymmetric problems to be examined here is that of an initially spherical bubble at rest in the vicinity of a rigid wall. There have been several previous investigations of this problem including the theoretical studies of Rattray[17], Shima[18], and Plesset and Chapman[7], and experimental studies for example by Ellis[19],

Kling[6], and Brunton[20]. The theoretical models are all for potential flow (inviscid), the first two being polynomial expansions which break down early in the calculated collapse because of the increasing deformation of the bubble. Chapman's dissertation presents a creative new approach to the problem although he does not compare his results with the other theoretical analyses or experiments.

One problem of this type has been solved here, that of an initially spherical bubble whose center is initially a distance b_o = 1.5 x R_o from a non-slipping approximately flat, rigid wall. The present use of spherical coordinates restricts boundaries of cells; therefore, a flat rigid wall (the solid line in Fig. 11) at 1.5 R_o from the bubble center must be simulated with a jagged wall coinciding with the boundaries of spherical cells (the dashed lines in the same figure). Actually such a boundary is quite similar to the roughness of a typical cast wall if the initial bubble diameter is about 1 mm, which is typical of many actual cavitation cases.

It should be noted here that collapse of a bubble initially spherical and with its center at a distance b_o from a flat rigid wall is essentially the same problem as the collapse of two identical initially spherical bubbles with their centers 2 b_o apart. The boundary condition at the plane of symmetry in the two bubble case, i.e., no flow across that plane, is the same as that at the rigid wall in the single bubble problem, except that the analogous wall condition would be that of full slip and zero shear at the wall. This analogy is often used (see, e.g., Ref. 6) in theoretical calculations of cavity collapse in the vicinity of a rigid wall and has also been affirmed by experiments with two spark-generated bubbles by Timm and Hammitt[21]. Fig. 12, taken from this reference, is a high-speed cinematographic sequence illustrating the resultant collapse.

The results of the calculations are shown in Figs. 11, 13, 14. Fig. 11 shows the bubble profile at several times during the collapse.

There is obviously an early elongation of the bubble normal to the wall; towards the end of the calculation (stopped by the singularity at the center of the coordinate system), the surface of the bubble appears to be returning to spherical. This is obviously only a transient situation, however, because the wall velocity at the top of the bubble (0^o) is much greater than elsewhere on the surface. Had it been possible to continue the calculation one would expect involution of the bubble from the top and, as Chapman[7] showed in the inviscid case, formation of a high velocity jet moving toward the wall.

Fig. 13(a) shows the mean radius of the bubble as a function of time and compares it with the case where no wall is present. The trend of the curve suggests that Rattray's[17] estimate of a 20% increase in collapse time at this initial distance from a rigid wall is quite appropriate. Fig. 13(b) shows the radial wall velocities along the 0, 90 and 180^o angles as a function of time. This figure shows the rapid acceleration of the liquid along the 0^o axis toward the end of the collapse, leading to the hypothesized conclusion reached above of involution and jet formation. Also, as in the "slip" velocity case, the velocity on the 0^o wall is rapidly approaching the magnitude necessary to cause "water hammer" damage.

Fig. 14 shows the pressure profiles along the three rays, 0, 90, and 180^o, at the end of the calculation, i.e., when $t = 0.873$ and $\bar{R}/R_o = 0.49$. One sees here that, along the 180^o axis, i.e., in the liquid between the bubble and the wall, there has been little pressure increase above ambient, in contrast to the situation on the opposite side of the bubble where the pressure grows rapidly due to inertial effects. This suggests that, at least at this initial spacing between the bubble and the wall, there is little chance that the pressure between the bubble and the wall is responsible for cavitation damage during collapse. This does not say however, that a shock wave arising during rebound of a gas and/or vapor-filled bubble could not be the source of

damage. This calculation does tend to confirm the theory that a high-velocity jet is an important source of damage.

Comparisons of the results of the present calculation with the recent theoretical work of Chapman[7] indicate a reasonably good agreement between the two in terms of profile histories and wall velocities as far as the present work goes, thus indicating that the effect of even the large viscosity used in the present calculation is small. Chapman's calculation goes on to show peak jet velocities (just before the liquid jet reaches the opposite side of the bubble) of 550 ft/sec, well above the damage threshold of many materials. Recent photographic studies by Brunton[20] indicate a jet velocity in a similar case of about 1800 ft/sec.

There is a real question as to whether a bubble at such an initial distance away from the wall (center at 1.5 R_o) is capable of causing damage. Both Ellis[19] and Kling[6] conclude from their experiments that there is not sufficient migration from this distance toward the solid surface during collapse, and hence that the jet velocity is attenuated by the water thickness adjacent to the wall, reducing the possibility of damage.

Since it has been shown experimentally on several occasions[22, e.g.] that only one out of a very large number ($> 10^4 - 10^5$) of bubbles appearing to collapse adjacent to a surface actually causes damage, it is evident that the specific initial conditions which give rise to damage are very restrictive. The bubble must migrate close to the wall, and the jet must not form until late enough in the collapse so that it will reach the opposite side of the bubble (and the necessarily adjacent wall) at precisely the right time to maximize the impact velocity.

It is now possible, with the aid of Figs. 15, 16, and the previously examined profile histories of Figs. 4, 5, 9, and 11, to determine the relative effects of the latter three asymmetries.

In terms of the eccentricity z ($z = (d_1 - d_2) / (d_1 + d_2)$), as

shown in Fig. 15, the effect of the pressure gradient $\sigma = 0.57$ is obviously the greatest while the $\sigma = 0.19$ pressure gradient and the slip velocity are less effective and very similar to each other in this regard. The rigid wall case is the only one in which the initial relative elongation is parallel rather than perpendicular to the axis of symmetry. Also to be noted here is that the value of z in the wall case minimizes and then returns rapidly toward zero and positive values characteristic of initial elongation and the involution normal to the wall. In Fig. 16, the pressure gradient cases are shown to have produced the greatest centroid migration, the slip velocity case the least.

The important fact to be drawn from these figures is that the effects of the three kinds of asymmetries examined therein are quite similar in that each is characterized by deformation and centroid migration of about the same magnitude and time scale and each of the three asymmetries produces bubbles which have involuted and formed high-velocity jets or, in the wall case, are about to behave in this fashion.

IV. CONCLUSIONS

Four different sources of asymmetry in bubble collapse in a viscous, incompressible liquid were examined; they include the effect of a slight perturbation from spherical symmetry and the effects on initially spherical bubbles of a pressure gradient, of a liquid velocity relative to the bubble, and of proximity to a rigid wall. The calculated collapse of the slightly perturbed bubble confirmed the "shaped charge" hypothesis of bubble collapse[23], that outward perturbations on the initial profile of a bubble will essentially involute as the collapse progresses, and also tended to confirm the instability of a spherical bubble surface during collapse in terms of growth of perturbations.

The effects of the other asymmetries on initially spherical bubbles were found to be remarkably similar to each other and on the same scale. In all three cases there was a substantial migration of the

bubble centroid from its initial position; in the pressure gradient and "slip" velocity cases there was also a flattening of one side of the bubble followed by involution and the formation of a relatively narrow high velocity jet of liquid. The bubble wall velocities around the surface in the solid wall case at the point the calculation was terminated were such as to produce a similar flattening, involution, and jet formation, had it been possible to continue the calculation. These asymmetries are produced with such small volume changes ($R/R_o > 0.25$) that we can assume that typical internal gas and vapor content of cavitation bubbles and moderate liquid viscosities would have no substantial effect on bubble collapse of this type.

The calculations indicated that, as one would intuitively expect, the steeper the dimensionless pressure gradient, the sooner flattening and involution will occur. Velocities of 220 ft/sec for still accelerating jets in cold water under a mean collapse overpressure of one atmosphere were obtained for pressure gradients typical under cavitation conditions and for collapse ratios $R/R_o = 0.2$. This velocity is sufficient to produce water hammer pressures greater than the yield strength of many structural materials. In the case of a bubble with slip velocity relative to the liquid, with a one atmosphere overpressure in cold water, a "slip" velocity of 5 ft/sec produces a jet velocity at the end of the calculation of 227 ft/sec.

In contrast to the pressure gradient and slip velocity effects, the initially spherical bubble near the wall (1.5 x R_o initial distance) first suffered a relative elongation along an axis normal to the wall. However, the bubble wall velocity at the point farthest from the solid wall continues to grow much faster than at other points on the surface, and based on similar results in the early stages of the other collapses, we can project eventual involution and jet formation in this case also. There is no buildup of pressure in the liquid between the bubble and the solid wall during the collapse, so this cannot be an important cause

of damage. Jet velocities and bubble profiles agree well with very recent calculations using a somewhat different approach by Chapman.[7]

A short motion picture film has been prepared from the computer results. Entitled "Computer Simulations of Asymmetric Bubble Collapse" by the present authors, this is available from the ASME Film Library.

V. ACKNOWLEDGEMENTS

Financial support for this study was provided under National Science Foundation Grant No. GK-13081.

BIBLIOGRAPHY

1. Lord Rayleigh, "On the Pressure Developed in a Liquid during the Collapse of a Spherical Cavity," Phil. Mag., Vol. 34, No. 200 (1917), 94-98.

2. Hickling, R., and Plesset, M., "Collapse and Rebound of a Spherical Bubble in Water," Phys. of Fluids, Vol. 7, No. 1, (1964).

3. Ivany, R. D., and Hammitt, F. G., "Cavitation Bubble Collapse in Viscous, Compressible Liquids -- Numerical Analysis," Trans. ASME, J. Basic Engr., 87 (1965), 977.

4. Ivany, R. D., Hammitt, F. G., and Mitchell, T. M., "Cavitation Bubble Collapse Observations in a Venturi," Trans. ASME, J. Basic Engr., 88, Series D (1966), 649-657.

5. Benjamin, T. B., and Ellis, A. T., "The Collapse of Cavitation Bubbles and the Pressures Thereby Produced against Solid Boundaries," Phil. Trans. Roy. Soc. Lon., A, 260 (1966), pp. 221-240.

6. Kling, C., "A High Speed Photographic Study of Cavitation Bubble Collapse," Ph. D. Thesis, University of Michigan (1970).

7. Plesset, M. S., and Chapman, R. B., "Collapse of an Initially Spherical Vapor Cavity in the Neighborhood of a Solid Boundary," Cal. Inst. Tech., Report No. 85-49 (1970); see also Chapman, R. B., "Nonspherical Vapor Bubble Collapse," Ph. D. Thesis, Cal. Inst. Tech. (1970).

8. Welch, J. E., Harlow, F. G., Shannon, J. P., and Daly, B. J., "A Computing Technique for Solving Viscous, Incompressible, Transient Fluid-Flow Problems Involving Free Surfaces," Los Alamos Sci. Lab., LA-3425 (1966).

9. Harlow, F. G., and Welch, J. E., "Numerical Calculation of Time-Dependent Viscous Incompressible Flow of Fluid with Free Surface", Phys. Fluids, 8 (1965), 2182-2189.

10. Mitchell, T. M., "Numerical Studies of Asymmetric and Thermodynamic Effects on Cavitation Bubble Collapse", Ph. D. Thesis, University of Michigan, 1970.

11. Mitchell, T. M. and Hammitt, F. G., "Collapse of a Spherical Bubble in a Pressure Gradient", ASME Cavitation Forum (1970), 44-46.

12. Plesset, M. S., and Mitchell, T. P., "On the Stability of the Spherical Shape of a Vapor Cavity in a Liquid", Quarterly Appl. Math., XII, No. 4, January, 1956.

13. Gibson, D. C., "The Collapse of Vapour Cavities", Ph. D. Thesis, Cambridge University (1967); see also Gibson, D. C., "Cavitation Adjacent to Plane Boundaries", Third Australian Conf. on Hydraulics and Fluid Mechanics, Sydney, 1968.

14. Hancox, N. L., and Brunton, J. H., "The Erosion of Solids by the Repeated Impact of Liquids", Phil. Trans. Roy. Soc. London, A, 260 (1966), 121-139.

15. Yeh, H. C., and Yang, W. J., "Dynamics of Bubbles Moving in Liquid with Pressure Gradient", J. Appl. Physics, 19, 7, June 1968, 3156-3165.

16. Chincholle, Lucien, "Etude de l'Ecoulement d'une Emulsion", These de Docteur es Sciences Physiques, Universite de Paris (1967).

17. Rattray, Maurice, "Perturbation Effects in Cavitation Bubble Dynamics", Ph. D. Thesis, Cal. Inst. Tech. (1951).

18. Shima, A., "The Behavior of a Spherical Bubble in the Vicinity of a Solid Wall", Trans. ASME, J. Basic Engr., 90, Series D, (1968), 75-89.

19. Ellis, A. T., "Observations on Cavitation Bubble Collapse," C. I. T. Hydrodynamics Lab. Report 21-12 (1952).

20. Brunton, J. H., "Cavitation Damage", Proc. 3rd International Congress on Rain Erosion, Farnsborough England, August 1970.

21. Timm, E. E., and Hammitt, F. G., "Bubble Collapse Adjacent to a Rigid Wall, A Flexible Wall, and a Second Bubble", to be presented at 1971 ASME Cavitation Forum.

22. Robinson, M. J., and Hammitt, F. G., "Detailed Damage Characteristics in a Cavitating Venturi", Trans. ASME, J. Basic Engr., 89, Series D (1967), 161-173.

23. Kozirev, S. P., "On Cumulative Collapse of Cavitation Cavities", Trans. ASME, J. Basic Engr., 90, D, No. 1, March 1968, 116-124.

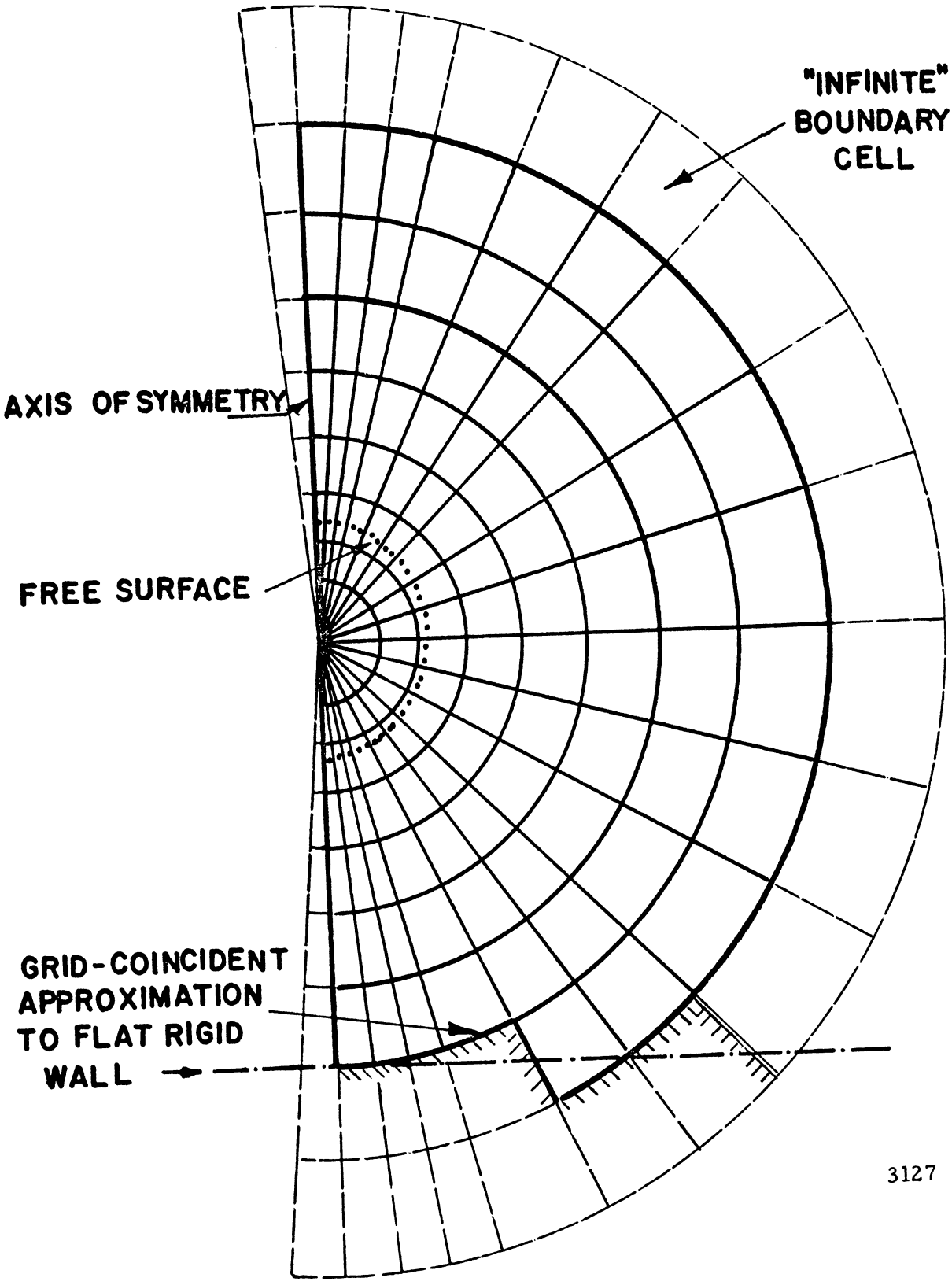

Figure 1. Grid, Initial Marker Particle Positions, and Boundary Conditions for a Marker-and-Cell Problem

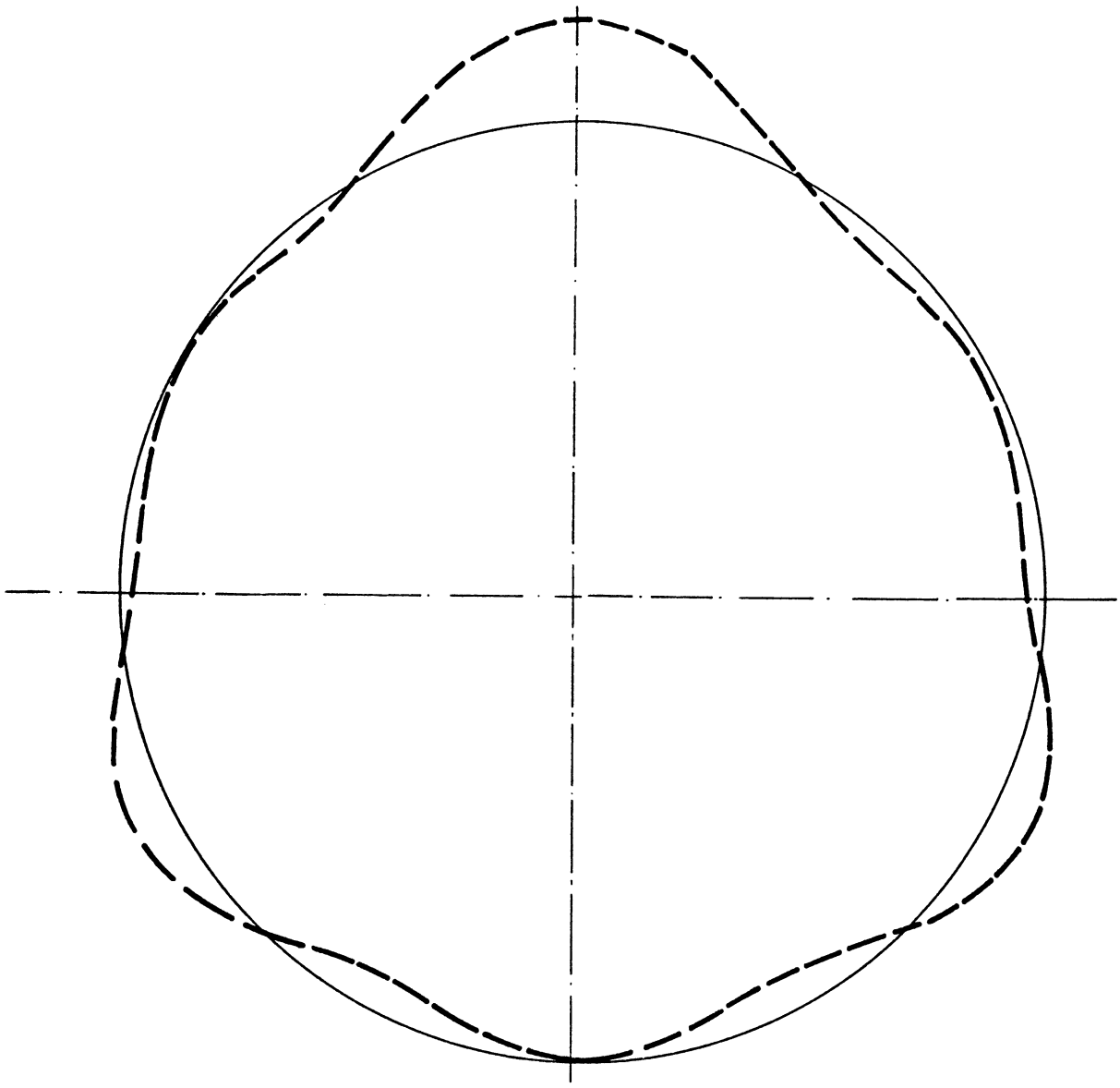

Figure 2. Initially Slightly Non-Spherical Bubble with Deviations from Spherical Magnified Ten Times

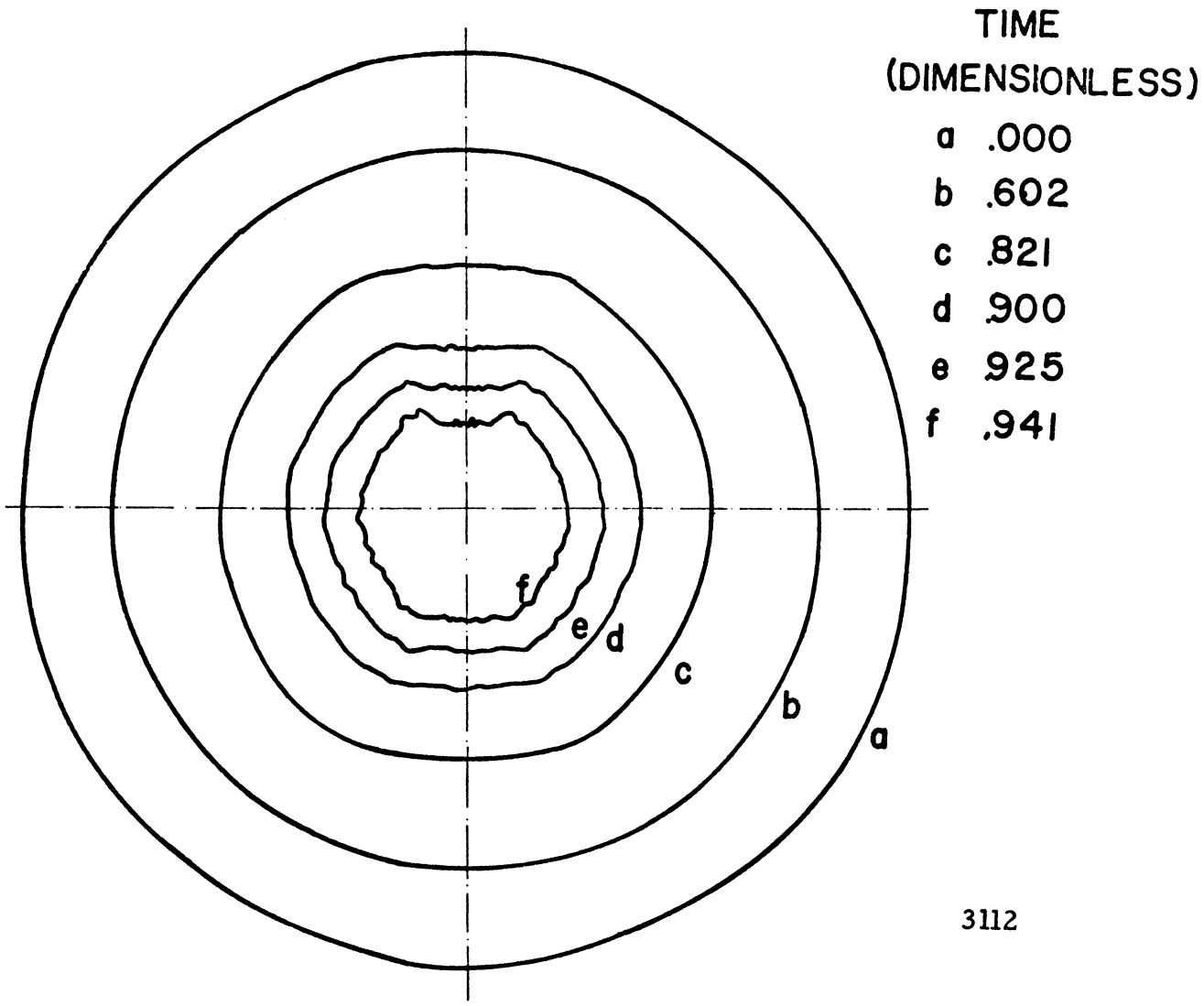

Figure 3. Bubble Surface Profiles for Initially Slightly Non-Spherical Bubble

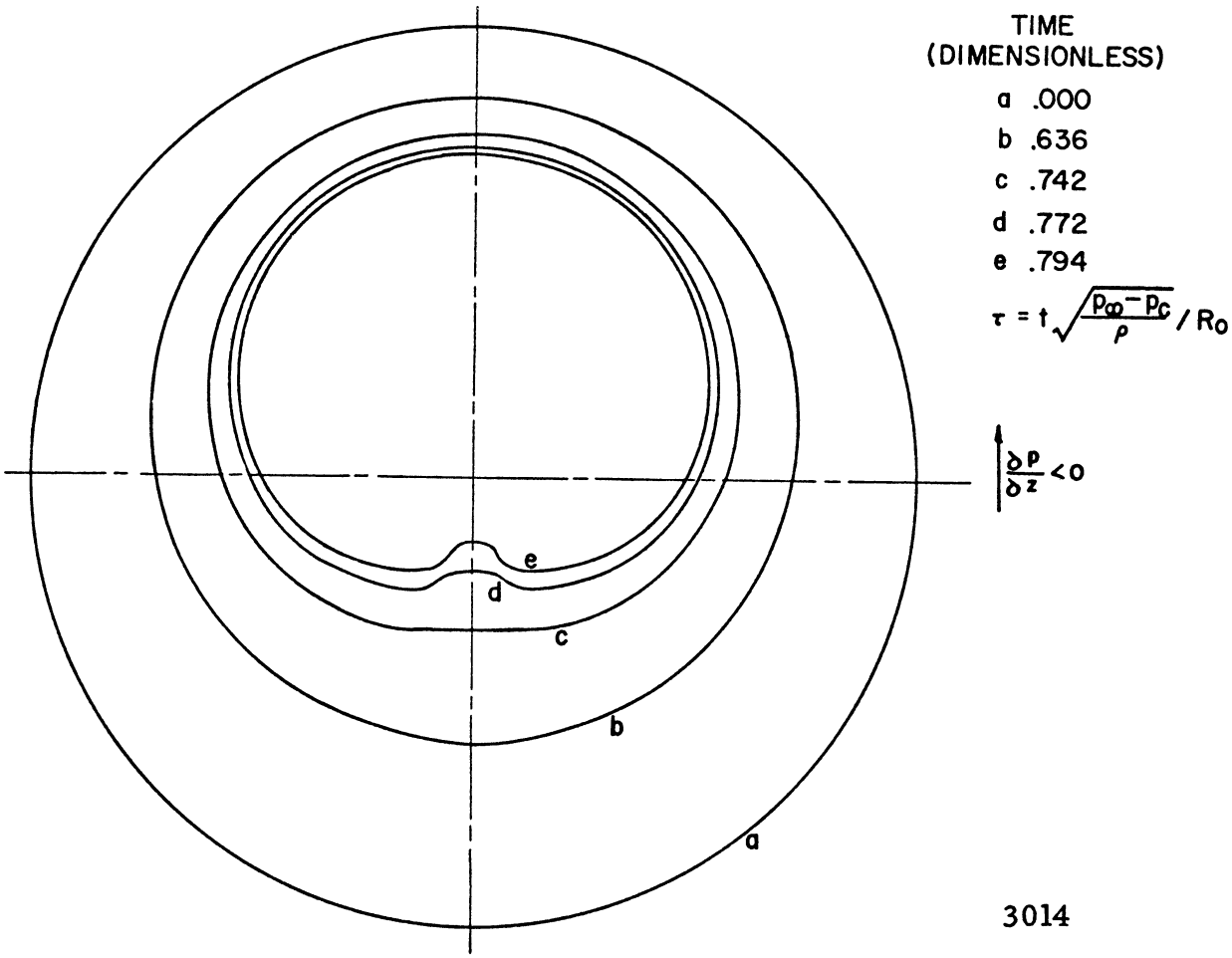

Figure 4. Bubble Surface Profiles for Initially Spherical Bubble in Linear Pressure Gradient, $\bar{\sigma} = 0.19$

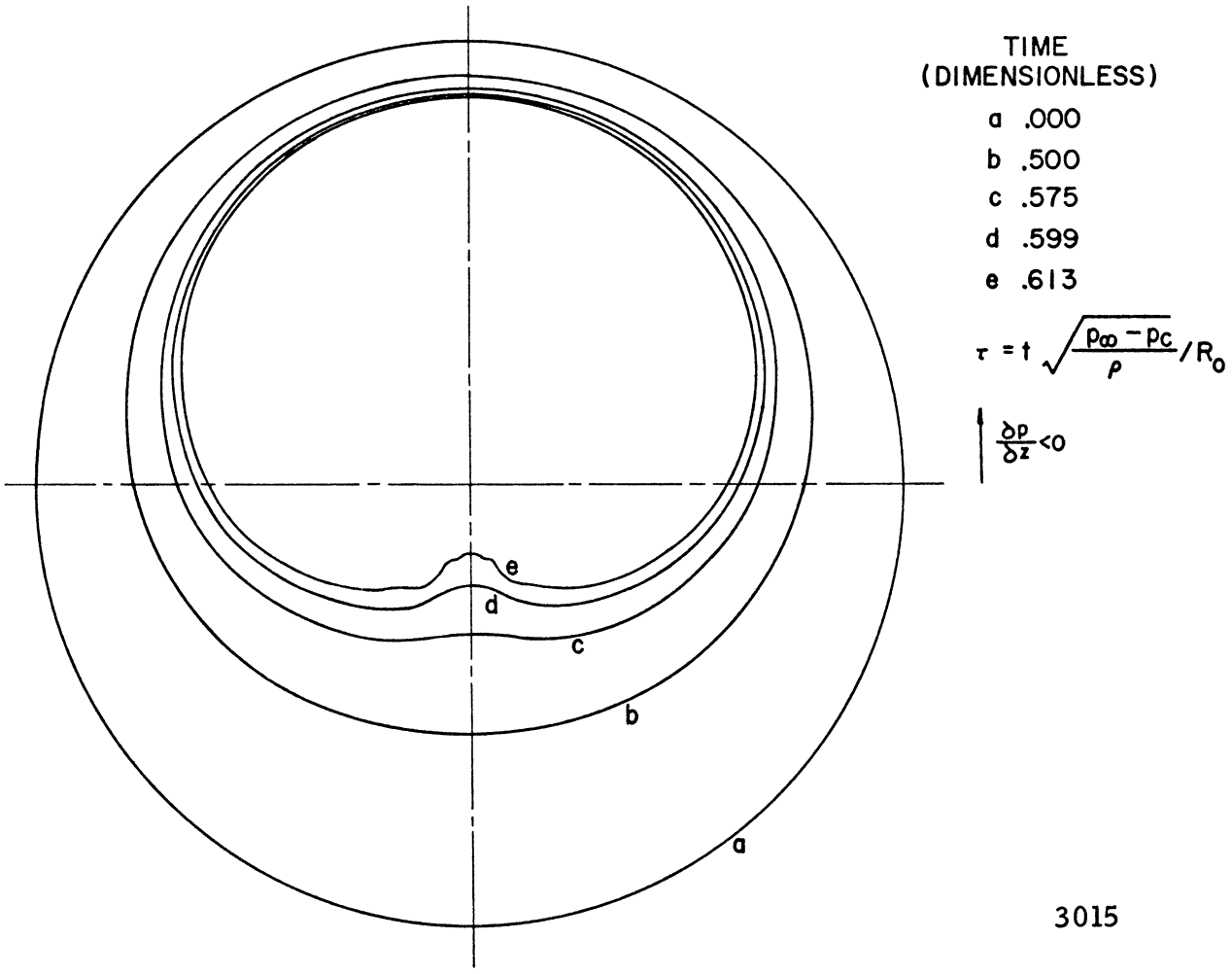

Figure 5. Bubble Surface Profiles for Initially Spherical Bubble in Linear Pressure Gradient, $\sigma = 0.57$

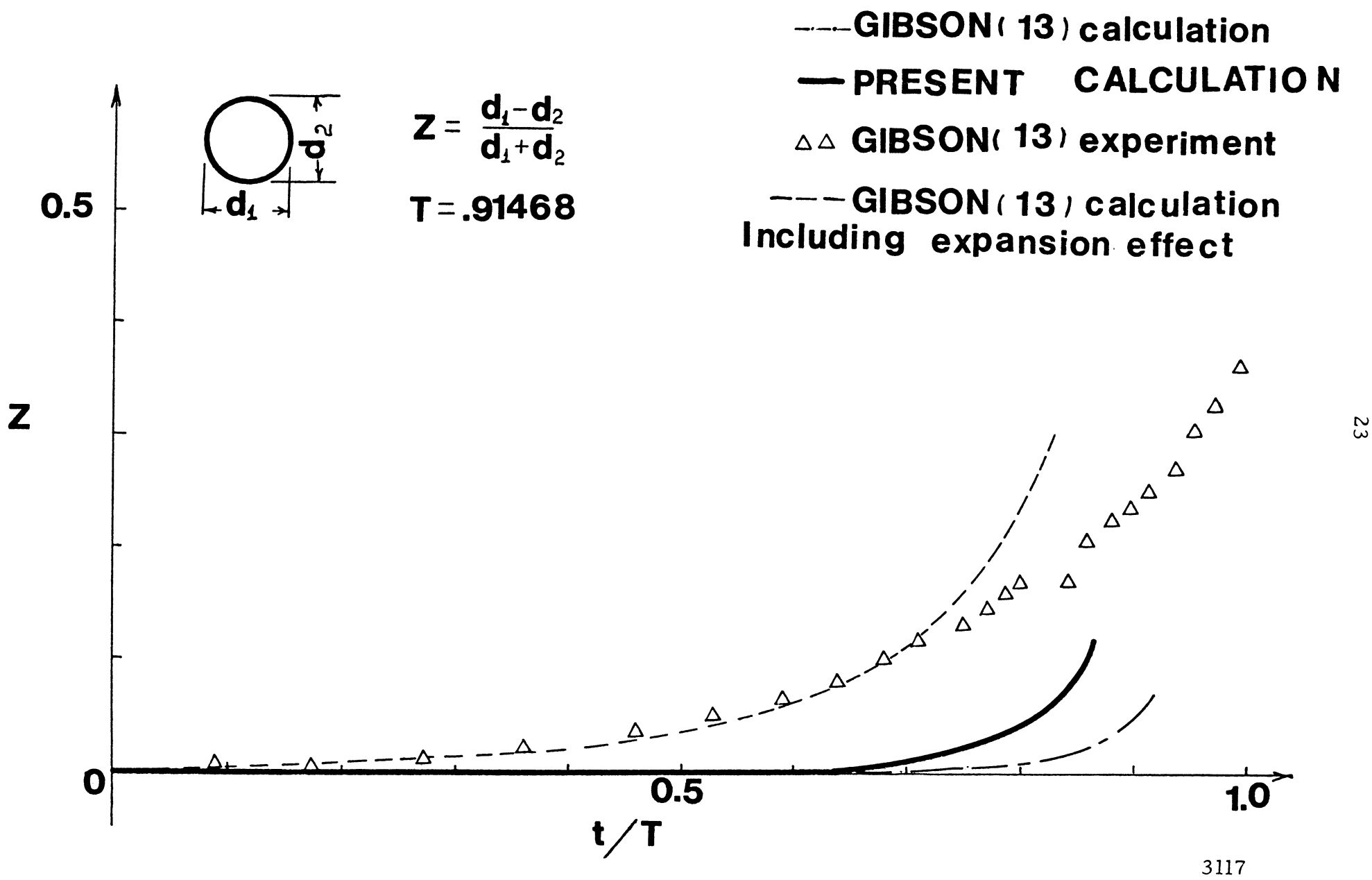

Figure 6. Comparison of Experimental and Theoretical Distortions of Initially Spherical Bubbles Collapsing in Linear Pressure Gradients, σ = 0.19

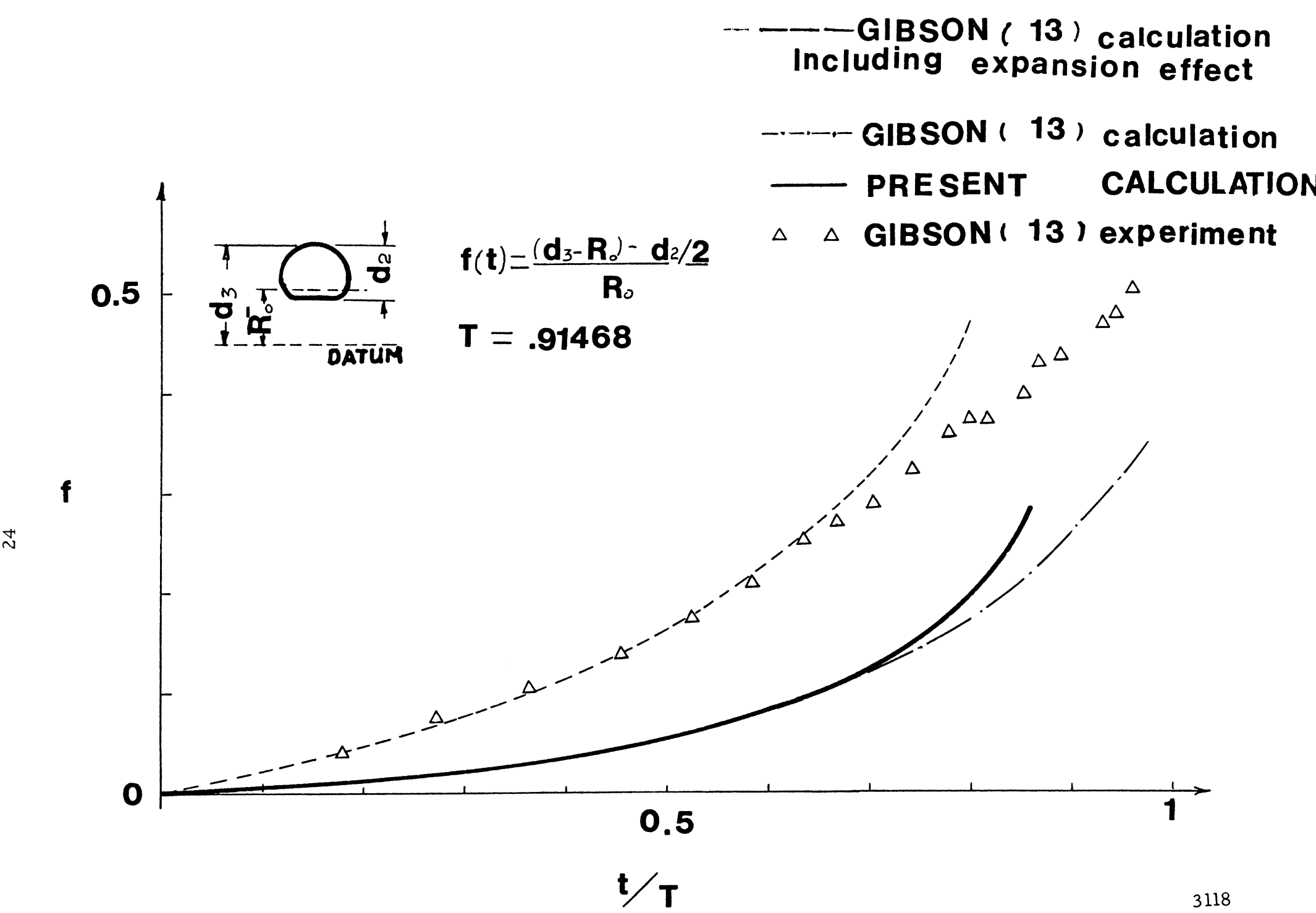

Figure 7. Comparison of Experimental and Theoretical Centroid Migrations

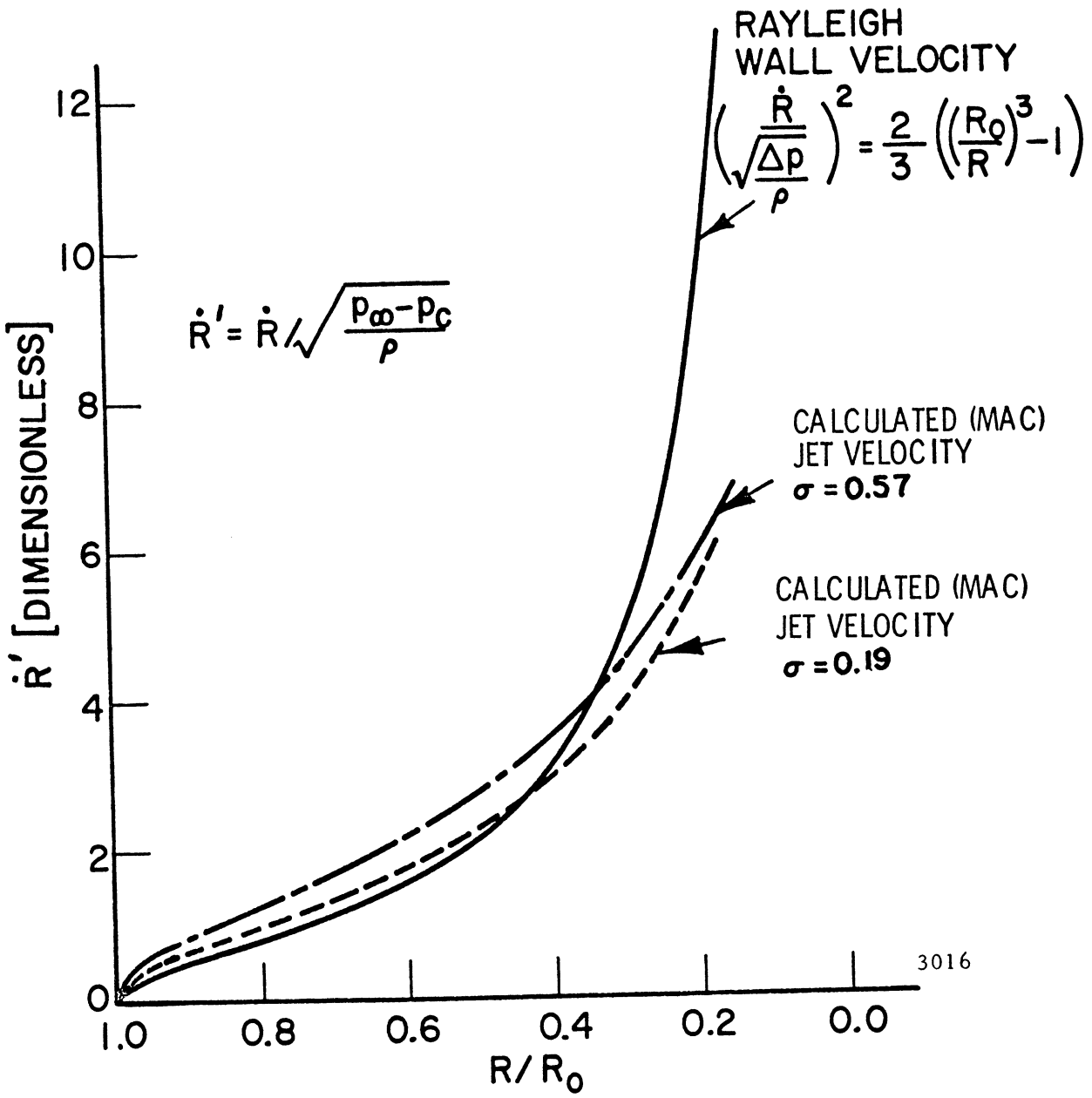

Figure 8. Jet Velocity as Function of Radial Position for Bubbles Collapsing in Linear Pressure Gradients

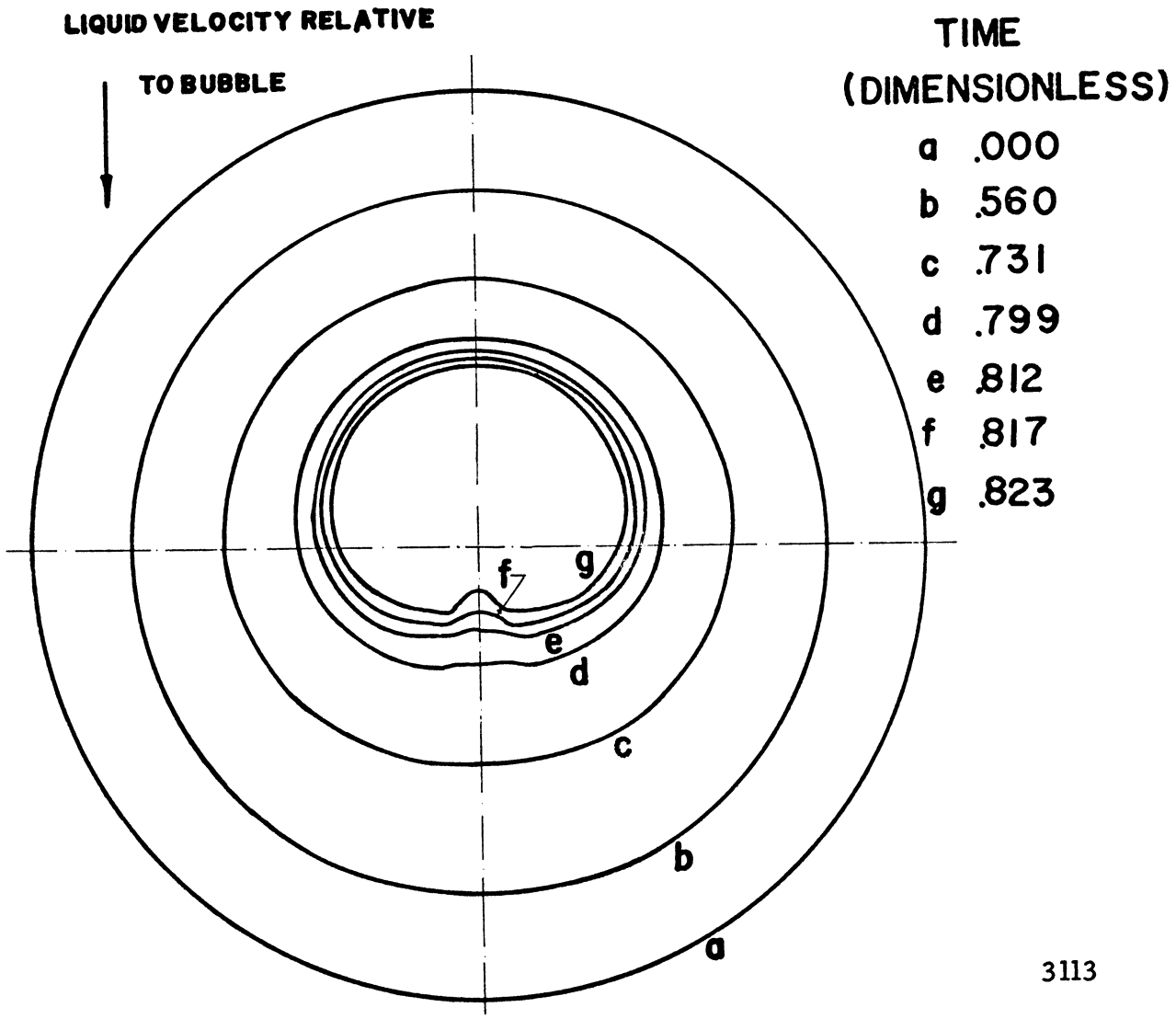

Figure 9. Bubble Surface Profiles for Initially Spherical Bubble Moving Relative to Surrounding Liquid, $V_{\infty} = 0.1515$

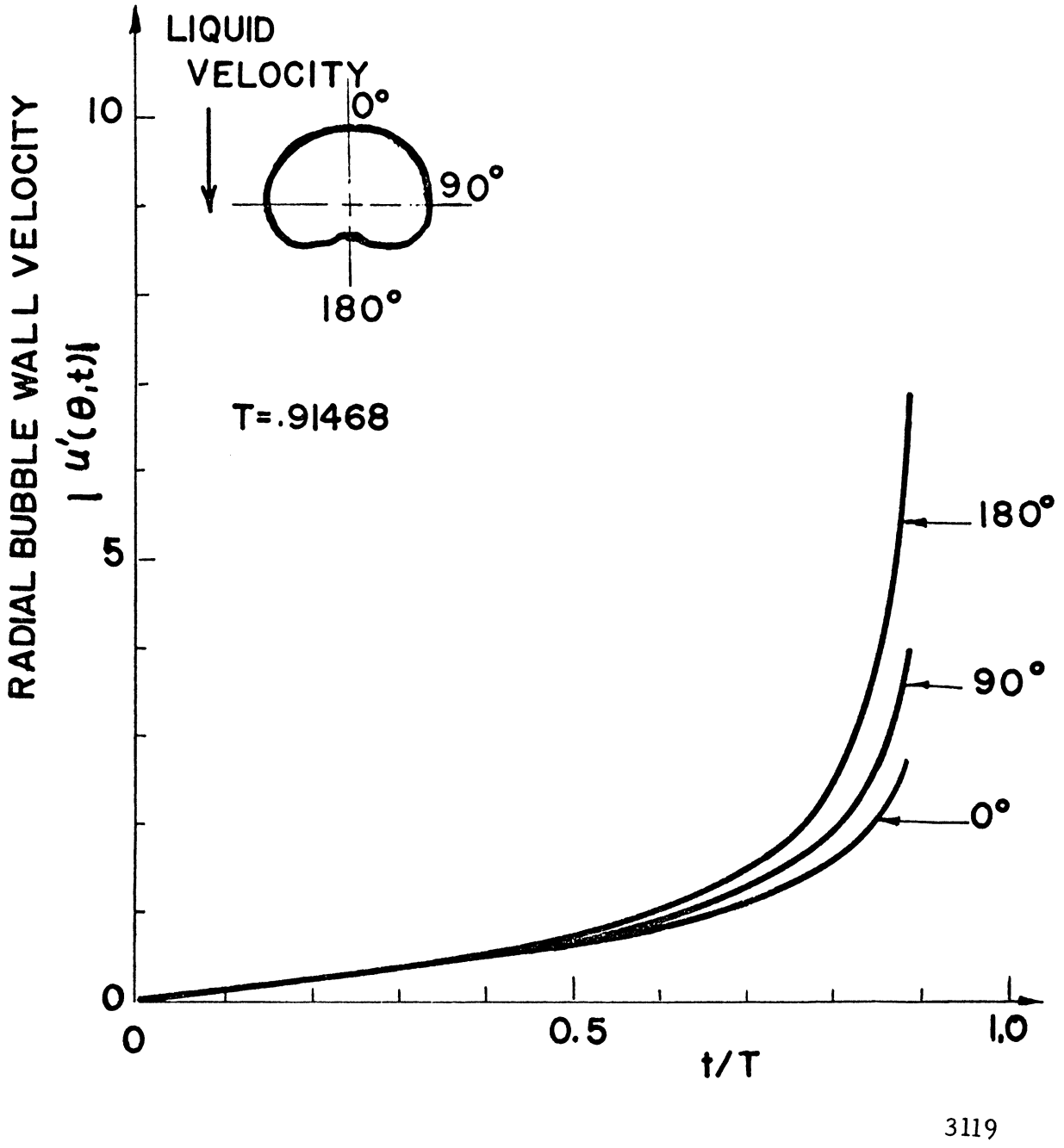

Figure 10.Bubble Wall Velocities at 0, 90, and 180° as a Function of Time for "Slip" Velocity Case

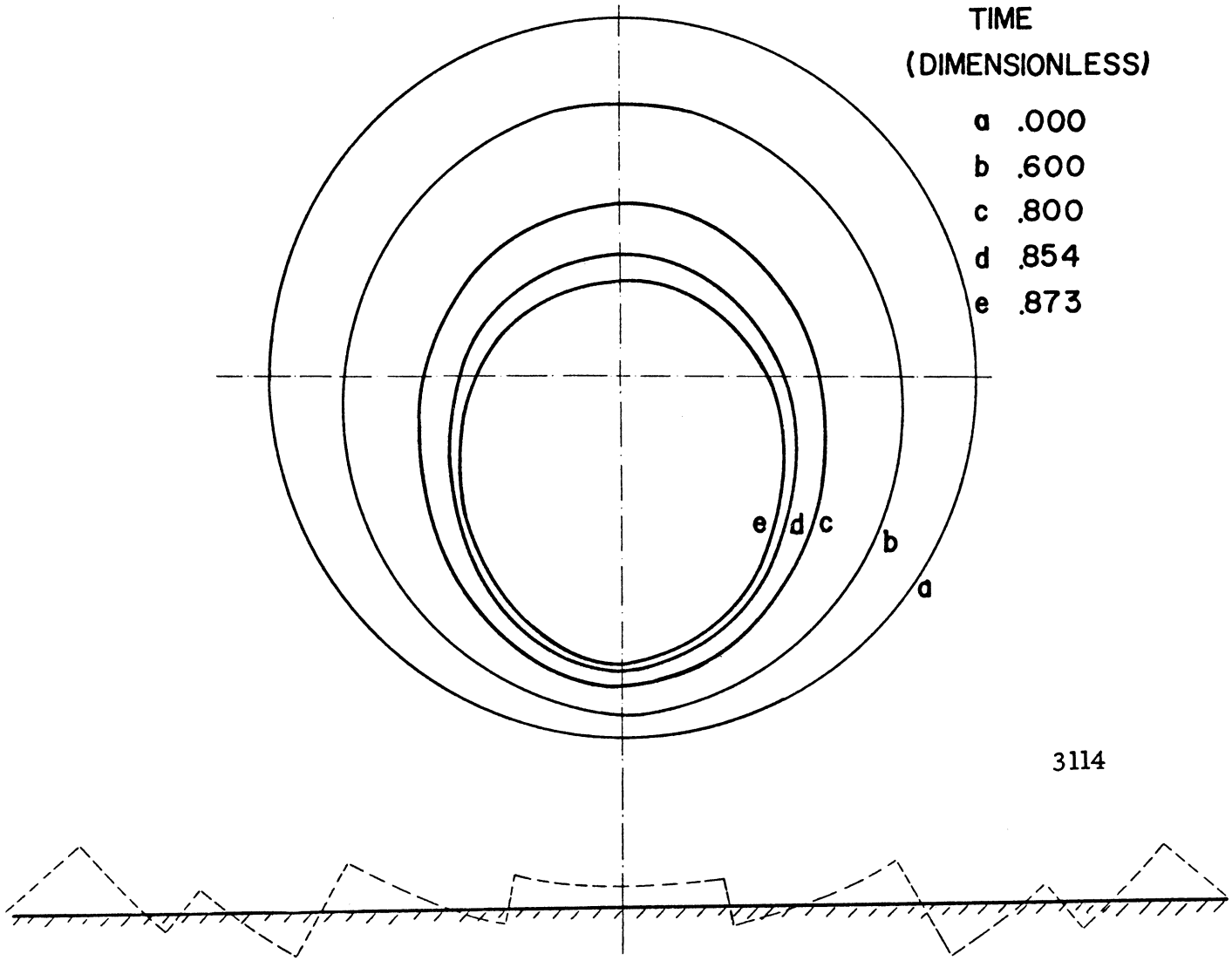

Figure 11. Bubble Surface Profiles for Initially Spherical Bubble with Center 1.5 R_o from Rigid Wall

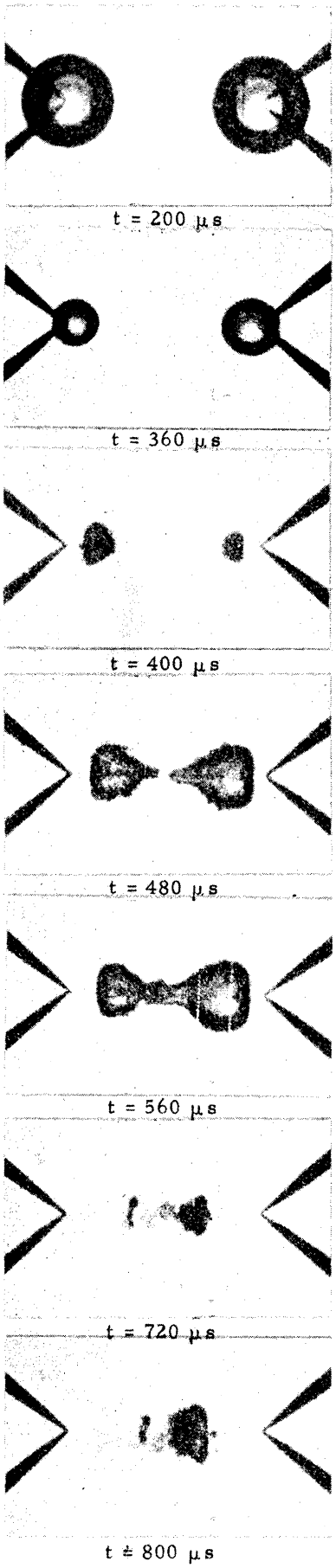

Figure 12. Two Spark-Generated Bubbles Collapsing Adjacent to Each Other

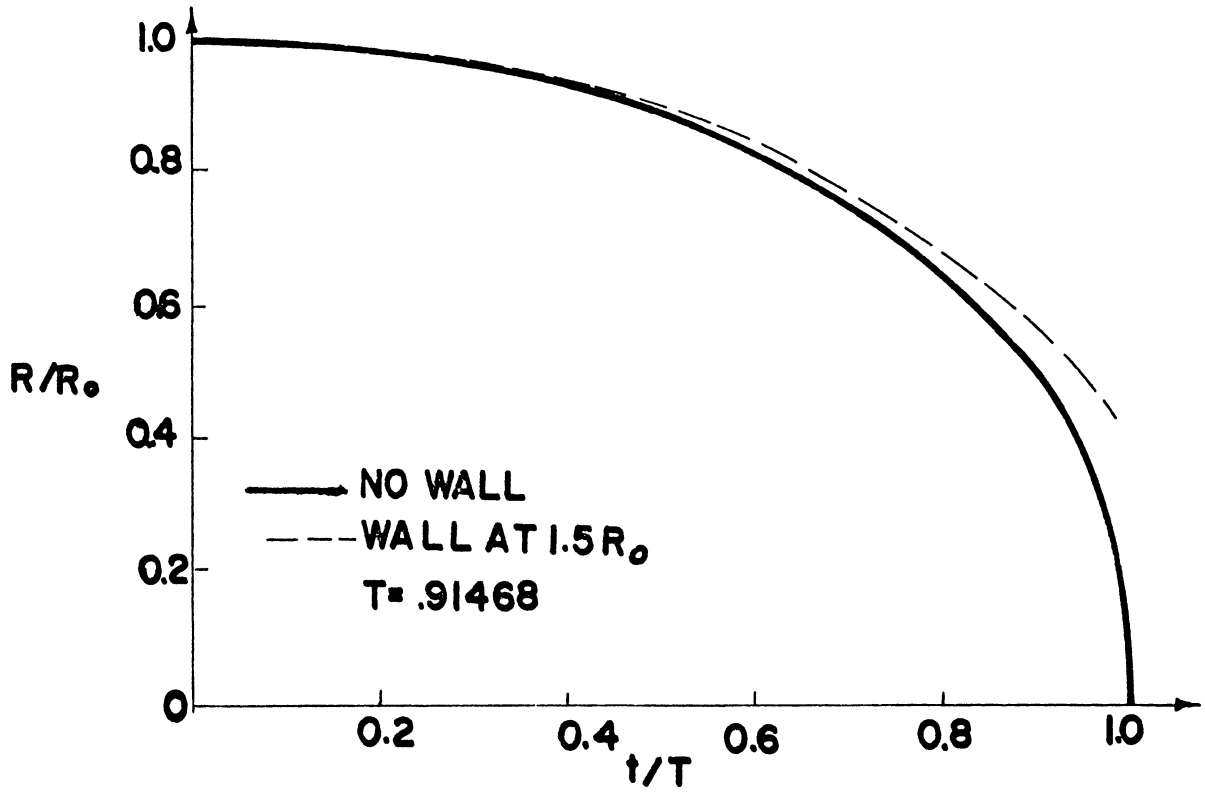

Figure 13(a). Mean Radius as a Function of Time with and without Rigid Wall

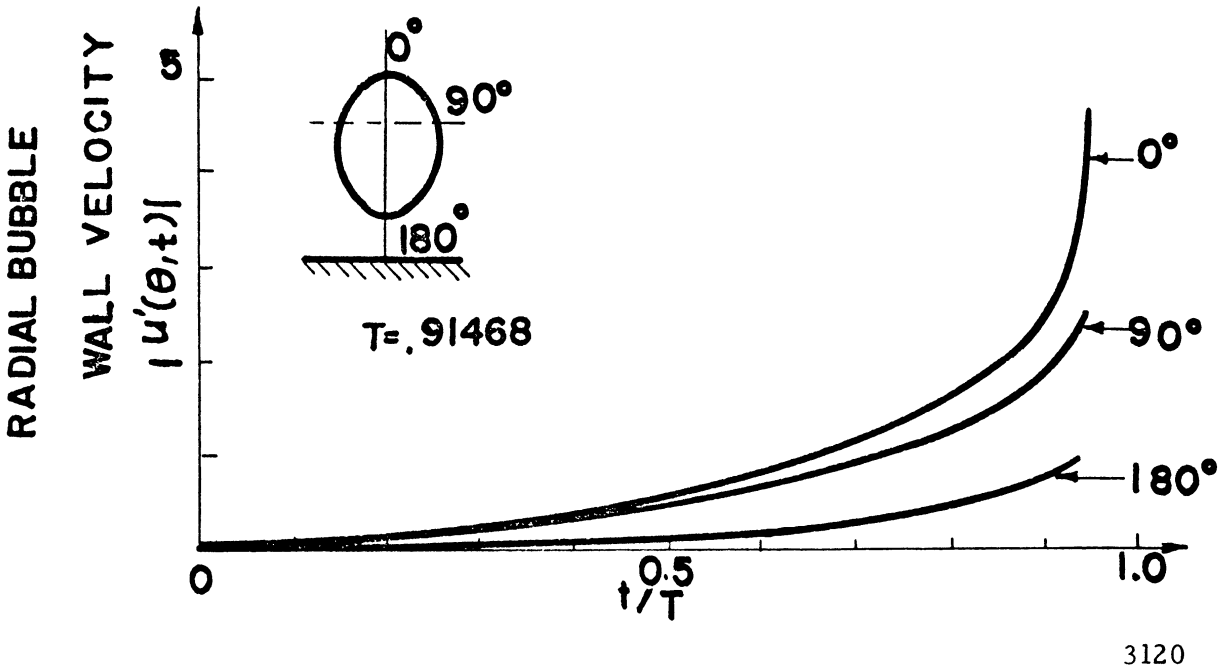

Figure 13(b). Bubble Wall Velocities at 0, 90, and 180° as a Function of Time for Wall Case

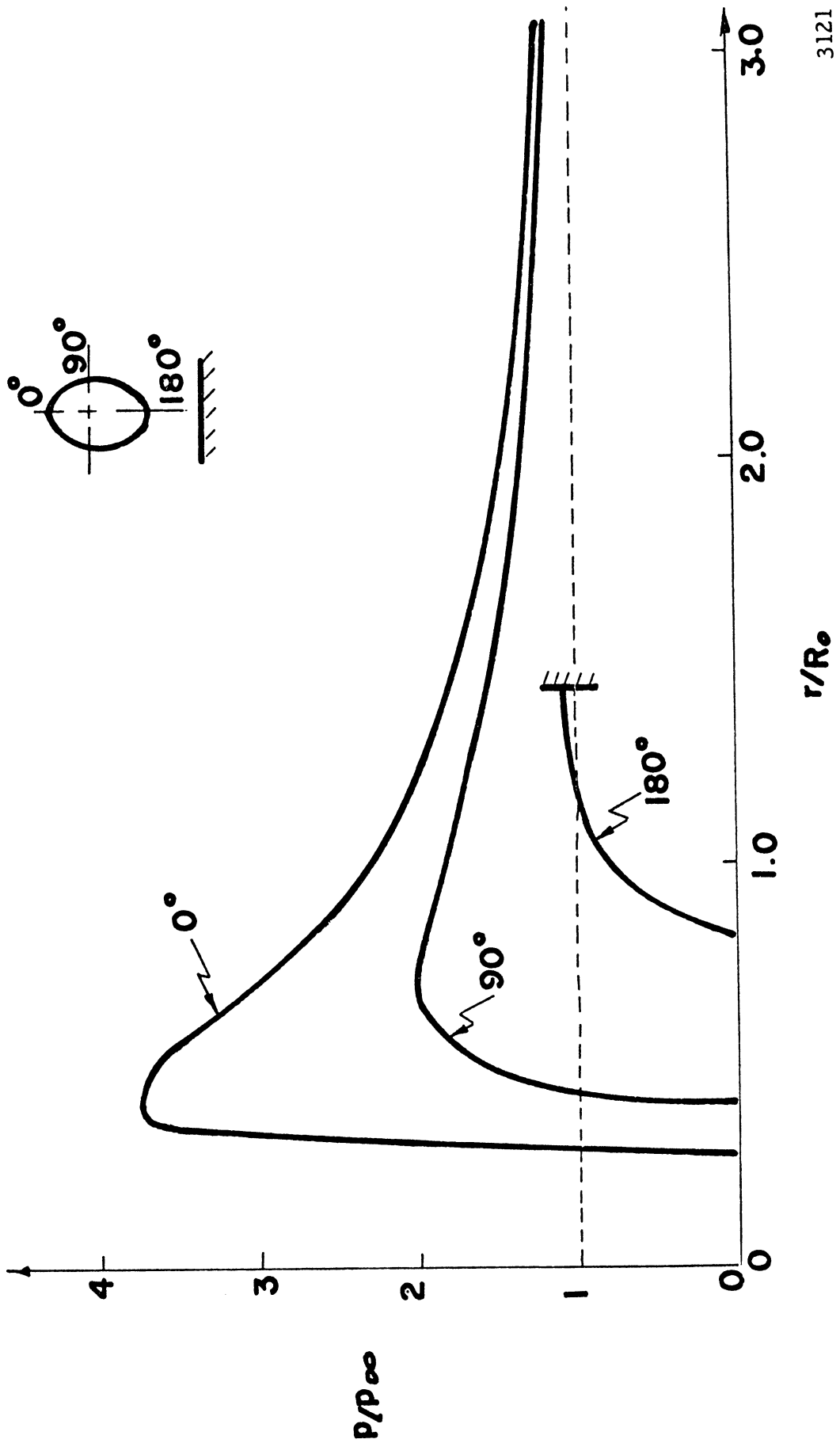

3121

Figure 14. Pressure Profiles in Liquid on 0, 90, and 180° Rays at $\bar{R}/R_o = 0.49$ for Wall Case

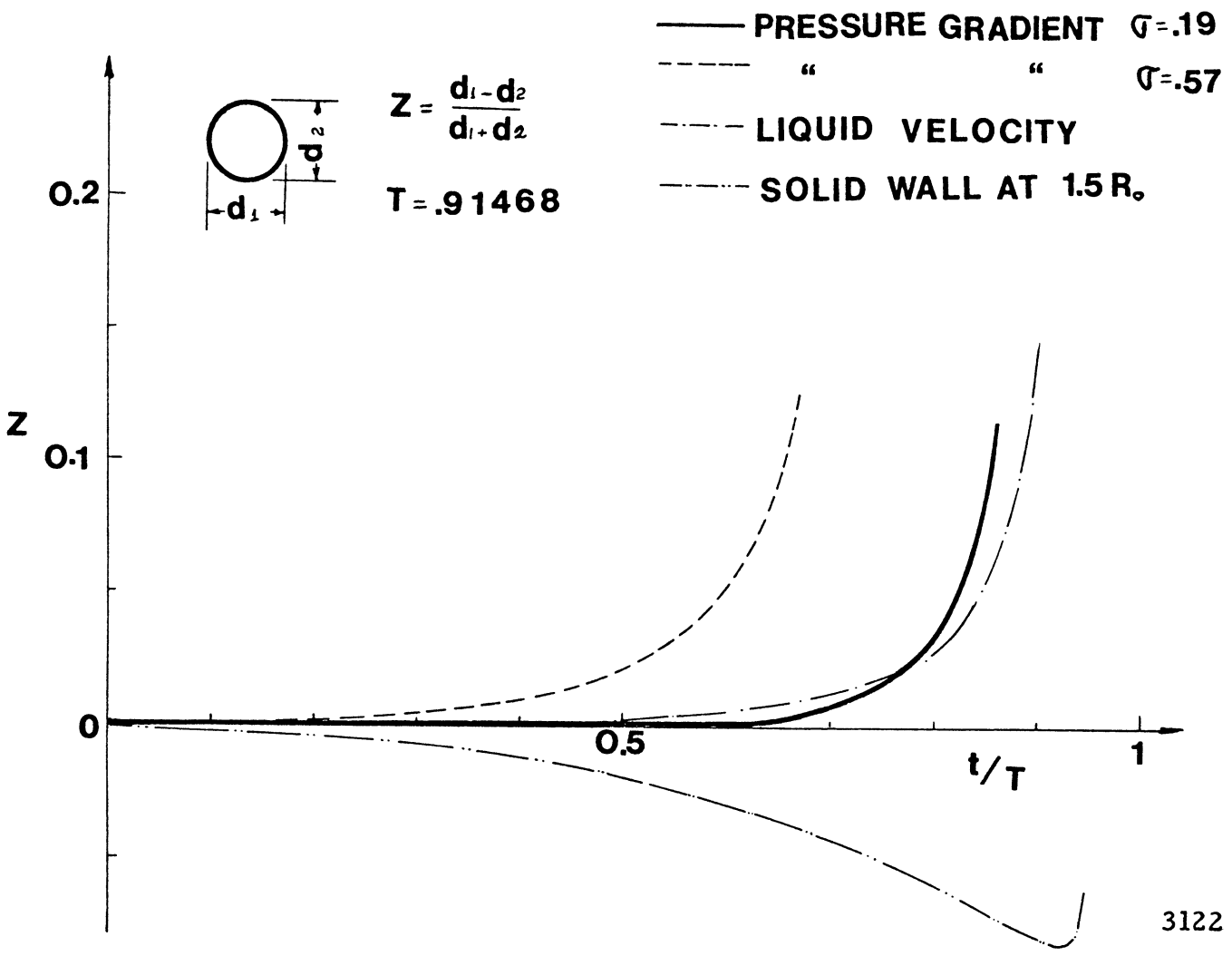

Figure 15. Comparison of Distortions of Initially Spherical Bubbles Collapsing under the Various Asymmetric Conditions